COMPREHENSIVE STUDY OF THE DELAMINATION OF GLASS-FIBER BASED COMPOSITES

Hocine Makri[1].*; Selma Baali[2]; Mohamed Slamani[3]
[1], [3]*Professor, Department of mechanical engineering, Faculty of technology, University of M'sila, Algeria.*
[1], [2], [2] *Laboratory of Materials and Structures Mechanics, University of M'sila, Algeria.*
[1]*Email:hocine.makri@univ-msila.dz* [2]*Email:selma.baali@univ-msila.dz.* [3]*Email:mohamed.slamani@univ-msila.dz*

***ABSTRACT**: In this paper, the effect of the winding angle and the number of folds on the delamination behavior of vinyl ester resin-fiberglass composites under mode-I loading was investigated experimentally. Accordingly, double cantilever beam samples with 8 and 12 folds and with different winding angles (±45°, ±55° and ±65°) were cut out of industrial pipes and subjected to mechanical tests. Furthermore, thick films were introduced during the winding process to create initial cracks of 50mm. The Mode-I fracture tests were conducted according to ASTM D5528-94a standards. Results show that the [±65°] winding angle provides the best delamination behavior and greater resistance to cracking compared to the [±55°] and [±45°] winding angles. Results also show that the number of folds has no effect on the initiation of the crack stage, but it significantly affects the propagation stage.*

***KEYWORDS**: Filament winding; Delamination; Composite pipes; Curved DCB specimens.*

1 INTRODUCTION

Laminated Glass-Fiber Reinforced Polymer (GFRP) composite materials are gaining wider acceptance in many sustainable infrastructure applications and the marine industry (Sathishkumar, 2014), thanks to their good environmental resistance, better damage tolerance, high specific strength and stiffness, high strength-to-weight ratio, low manufacturing cost, as well as excellent durability and corrosion resistance (Baali. B, 2020). They are already used instead of conventional materials in numerous products and industrial applications (Simon, 2014). Glass-Fiber Reinforced Polymer (GFRP) Composites are used as pipes for underground civil applications such as, sewer and wastewater evacuation because they offer considerable advantages compared to metallics in terms of high compression resistance, low manufacturing and maintenance costs, electrical insulation, excellent durability, and no need for any form of corrosion prevention. Unfortunately, they are more damage-sensitive than metallics when subjected to loads. Generally, this damage arises as fold separation, called delamination, which is the most frequently encountered type of damage in these kinds of laminate composites. Usually, this undesirable behavior leads to a significant decrease in the rigidity and strength of structures and then to a possible completes failure (Nageswara, 1995). Additionally, the stresses generated by the external loadings cause delamination in the curved regions of the GFRP pipes. Consequently, the study of delamination propagation in curved structures has become of great importance in engineering (Ghadirdokht. 2019).

Several types of delamination can occur in a composite structure, depending on the loading conditions. Mode-I refers to a loading manner that induces strand opening; mode II induces forward shear; and mode III induces anti-plane shear. Furthermore, the resistance of the composite material to delamination at each loading mode is often quantified in terms of the interlaminar fracture toughness. This is usually expressed by its corresponding critical energy release rate, GIc, GIIc, and GIIIc, respectively (Raju, 2008). Because mode-I delamination presents the lowest fracture energy and produces the most damage, it is retained as a measure criterion for the damage tolerance of structural polymer composite parts (Mahmoudi, 2014). The ASTM standards (ASTM D5528, ISO/DIS 15024) recommend the Double Cantilever Beam (DCB) test as the common method for the characterization of the mode-I delamination (interlaminar fracture toughness) in flat composite specimens (Szekrényes, 2005).

The mechanical behavior of composite pipes is influenced by several parameters, such as the volume fraction of fibers, the number of folds, the ply thickness, the sequence of plies, the winding angle, and the yarn width (Jia, 2013), (Rafiee, 2013 &Yang, 2016). Davies et al. (Davies, 1994) and Ozdil et al. (Ozdil 1999), have experimentally studied the influence of curvature on the delamination of tubes manufactured by a filament

winding process. By comparing GIc values for samples cut from filament wound tubes (cut parallel to the tube axis) with those cut from flat filament wound unidirectional glass fiber reinforced composite plates, Davies et al. observed no variation in GIc values for both samples, unlike Ozdil et al. who found a small influence of curvature on GIc and complacency (C) values. Ozdil et al. (Ozdil, 1999), (Ozdil, 2000), also specify that this influence can be reduced by increasing the laminate thickness. Davies (Davies, 1989) and Leonard et al. (Leonard, 2009), investigated the influence of the fiber content on the delamination behavior of laminates for carbon fiber reinforced epoxy composites. Davies and Benzeggagh used 61% of the fiber volume fraction, while Leonard gradually increased the fiber volume fraction from 12% to 60% by a step of 12%. In both papers, the ASTM standards were used to determine the energy under mode I loading. Their results show a significant increase in the fracture toughness and critical energy release rate attributed to the fiber bridging formed behind the crack tip. Mahmoudi (Mahmoudi, 2014), noticed the effect of fiber bridging on the enhancement of GIC values.

The effect of fiber orientation on the delamination of laminar composites has been of interest to several researchers, such as Shetty et al. (Setty, 2000) and Mertiny et al.(Mertiny, 2004); They concluded that a variation of the fiber orientation angle with respect to the direction of crack propagation provided high fracture toughness and durability.

The influence of the stacking sequence and the fiber orientation on the strain energy release rate GIc was investigated by Julias et al. (Julias, 2018), Davallo. (Davallo, 2010) and Szekrényes et al. (Szekrényes, 2005) for a variation from 0° to 90° of the fiber orientation of the four layers near the mid-plane. Julias et al. obtained a GIc enhancement of 50%, which is attributed to fiber bridging and fiber pull-out. But they attributed the enhanced crack propagation along the fiber surface to the coincidence of the fiber direction with the crack direction. Whereas, Davallo attributed the amelioration of the GIc and GIIc values to the reinforcement mechanisms such as interfacial debonding and fiber bridging. Szekrényes et al. (Szekrényes, 2005), confirm the contribution of fiber bridging to the resistance to delamination improvement. Moreover, they connect the energy release rate increase with the crack length, known as the R-curve effect. Several studies related to the delamination of laminar composites can be found in the literature. Furthermore, most of them are carried out on DCB specimens exhibiting a longitudinal curvature (Davallo, 2010), (Aslan, 2020), (Wróbel, 2017), and (STANDARD, A. S. T. M, 2011). However, the delamination of DCB specimens with curvature in the width sense has never been investigated. In fact, this is one of the important issues that must be addressed in order to better understand the delamination behavior in the composite tubes.

The main objective of this work is therefore to study the delamination growth in DCB specimens with curvature in the width sense. Accordingly, many specimens cut from vinyl ester resin-fiberglass industrial pipes commonly used for sewer and wastewater evacuation applications are prepared and used in this study. Furthermore, the effect of the winding angle and the number of plies on the delamination behavior was also investigated in this paper.

2 EXPERIMENTAL PROCEDURES

2.1 Materials

The materials used in this study are GFRP composite pipes made from vinyl ester resin as an impregnating agent and a continuous E-glass fiber roving (E6-type) with 2400 Tex of type EDR24-2400-38 as reinforcement. These materials are supplied by Maghreb Pipe Company (a local company). The vinyl ester is a thermosetting usually used for composite manufacturing purposes such as storage tanks, pipes, hoods, ducts, and exhaust stacks because of its superior mechanical properties such as corrosion resistance, processability parameters, and toughness higher than polyester resins (Rao, (2017).

The mechanical properties of the resin used were determined by tensile and bending tests and are as follows: limit flexural strength ~150 MPa (ISO 178), flexural modulus 3.8 Gpa, limit tensile strength ~85MPa (ISO R527), and Young's modulus 3.3 Gpa (ISO R527). The characteristics of roving were provided by the supplier as follows: Fiber diameter ~24 µm, density 2.54 g/cm3, tensile strength 2741 MPa, Young’s modulus 81,232 GPa, Poisson ratio 0.22, and elongation 4%.

2.2 Pipes manufacture

The pipes used in the experiment were manufactured by the filament winding technique, as illustrated in Figure 1. It consists of a continuous glass fiber roving, impregnated with a mixture of thermosetting resin and a catalytic system, wound around a rotating mandrel. The GFRP pipe is obtained by the adjustment of two movements, respectively, the rotation of the mandrel and the

alternative movement of the glass band guide. After shaping by filament winding, a thermal cure at 150°C for 30 to 40 minutes is necessary while maintaining the rotation of the mandrel.

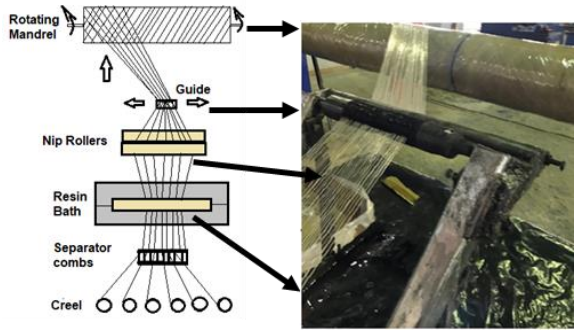

Figure 1. Filament winding process.

Three winding angles were considered during the manufacture of the tubes (±45°, ±55° and ±65°), with 8 and 12 ply for each winding angle. These winding angles were chosen because they provide the best usage characteristics (Mertiny, 2004), (Suresh, 2016). Furthermore, a non-adhesive Teflon film, Polytetrafluoroethylene (PTFE) of 13mm thickness, is inserted in the central layer during manufacture (Figure 2). This Teflon film acts as a delamination initiator, assuring the initiation of a crack in the midlayer during loading (Rafiee, 2013).

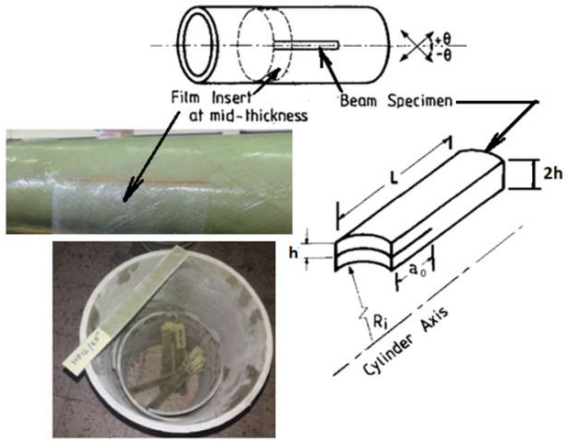

Figure 2.Test specimen preparation and film inserted at midlayer.

2.3 Specimens preparation

Specimens were cut out of GFR pipes with an inner diameter of 500mm. A total of three test specimens were cut for each fiber orientation using a diamond disc saw. The dimensions of the specimens were chosen according to the ASTM D5528-94a standard (Rafiee, 2013). They are 200mm in length, 25mm in width, and 5±0.2mm in thickness, with initial crack lengths of about a_0=55 ±0.2mm. Furthermore, their surfaces were scrubbed with sandpaper and cleaned carefully. The edges were first flat polished prior to bonding the loading blocks with the araldite adhesive onto the two sides of the specimen (Figure 3).

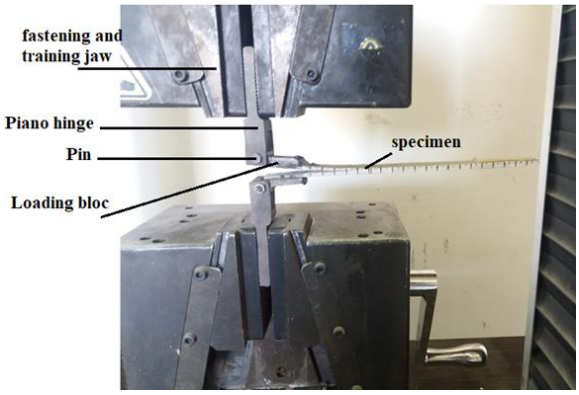

Figure 3. Experimental device used for delamination test

2.4 Mode I interlaminar fracture test

The Mode-I fracture tests were conducted at 20°C according to ASTM D5528-94a and ISO 15024 standards (Prasad, 2011), (Gunderson, 2007), using a Universal Testing Machine (INSTRON-5969) equipped with a force sensor. The loading capacity of this machine is 50 KN. In order to realize fully crack-opening loads during the tests and avoid moments at the loading point, the load has to be applied in such a manner that the force remains perpendicular to the specimen face. To achieve this task, a pair of metallic blocks was glued to the end of each specimen (Figure. 3). All failure tests were performed at a crosshead speed of 1 mm/min, during which the collected force-displacement (P – δ) values were recorded. An LCD camera connected to a computer is placed in front of the testing machine, allowing the observation and acquisition of instantaneous images and thus facilitating the follow-up of the crack propagation during the entire testing period. The estimation of the size of the initiated cracks that propagate during loading is obtained by drawing an equidistant line of 1mm along the edges of the tested specimen. Furthermore, parts of the specimens recovered after testing were cut out, and their edges were examined using a microscope equipped with a camera and image processing software.

.The Compliance Calibration (CC) Method is used to determine the critical energy release rate in Mode-I according to the following formula (Equation. 1):

$$G_{IC} = \frac{nP\delta}{2ba} \quad (1)$$

where n is an exponent, which can be calculated from the slope of the log-log plot using the visually

observed delamination onset values and all the propagation values.

The compliance, C=δ/P, is calculated through experimental data. It can be expressed as follows:

$$C = ma^n. \quad (2)$$

Where n represents the slope of the log-log plot of crack length and compliance and can be determined from the following formula:

$$LogC = nLoga + Logm \quad (3)$$

2.5 R-curve

The R-curve describes the evolution of the delamination resistance or fracture toughness as a function of the crack length. The relation between the effective crack length and the interlaminar propagation energy is determined by the law of compliance as follows:

$$G_{Ip} = \frac{nP_c^2}{2bk} a_{eff}^{n-1} \quad (4)$$

3 RESULTS AND DISCUSSIONS

The glass volume fraction of the pipes used in these tests is determined experimentally by the burnout test. The volume fractions were found to be about 67.52 percent for the 8-fold pipes and 67.64 percent for the 12-fold pipes. These values are superior to the nominal values initially set at 55% by the supplier of the pipes. According to previous studies (Davies, 1994), (STANDARD.A.S.T.M, 2011), this relatively small variation in the volume fraction did not affect the interlaminar GIc values appreciably.

3.1 Mechanic tests

The mode-I fracture mechanics test was carried out on DCB specimens under displacement control mode. Results show that in all of the tested specimens, crack growth occurred at the crack starter in the mid-plane of the beams. According to the collected data of the force-displacement (P-δ), three load-displacement curves have been plotted in Figures 4 and 5.

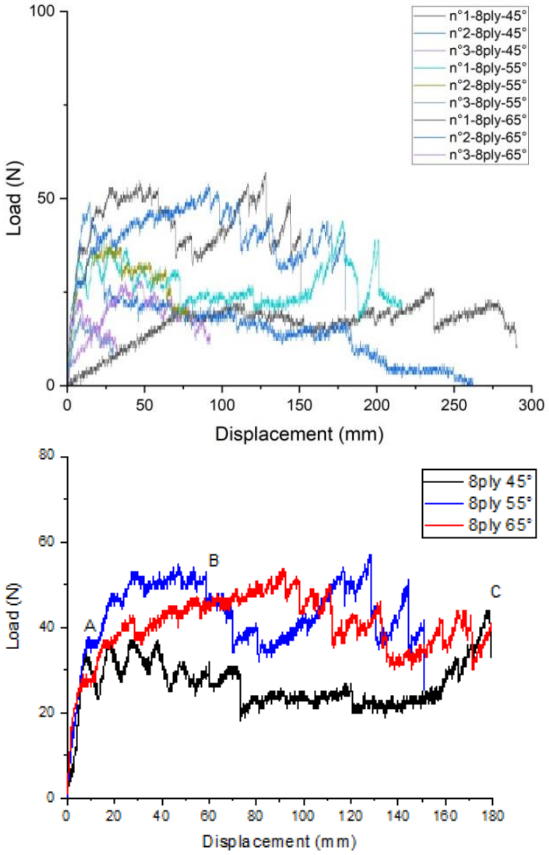

Figure 4. Load-displacement curves for 8-ply specimens: All curves, b) Representative curves.

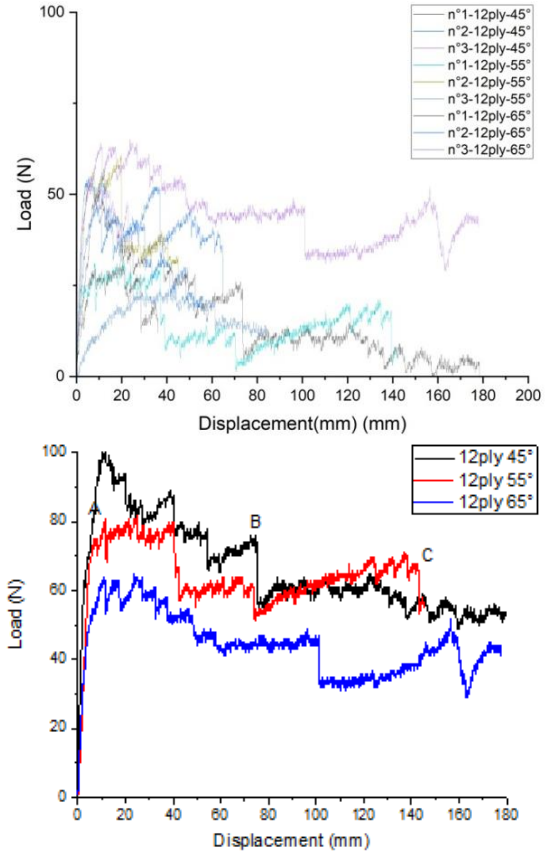

Figure 5.Load-displacement curves for 12-ply specimens: a) All curves; b) Representative curves.

It can be seen from these figures that the three curves have almost similar shapes and can be divided into three major parts: A, B, and C. Part A is called the elastic region of the curve. This region exhibits a linear trend, in which the load increases linearly with the displacement. It can also be seen in this region that the linear aspect is disturbed by small peaks. This can be explained by the fact that the fibers and the matrix have different properties. The end of the linearity (point A) corresponds to the crack initiation. The second part of the curve (AB) exhibits an increase in the load versus displacement until point B, followed by a continuous release until point C. Fibers bridging occurs at the crack tip between the strands of the tested specimens. This phenomenon is suspected to be the origin of the noticed increase in the GIc values. This finding is in agreement with previous studies (Davies, 1989), (Davallo, 2010). The third part of the curve (BC) shows a decreasing slope disturbed by peaks, represented by a non-linear behavior like a 'stick-slip' with delamination growth. This behavior can be explained by the fact that the crack jump between interfaces causes translaminar cracking (Ghadirdokht, 2019). Furthermore, the decreases in load observed with increasing crack growth observed in curves correspond to a stable propagation of delamination due to the rupture of the bridged fibers mentioned previously.

3.2 Determination of the intrinsic parameters of the material

The applied load and displacement values available for various crack lengths allow plotting the curves of compliance depending on the delamination growth according to formula 3. Accordingly, linear curves are obtained and represented in Figures 6 and 7, respectively. Where n is the slope of the linear curves. The values of the intrinsic parameters (n and m) of the material deduced are regrouped in Table 1.

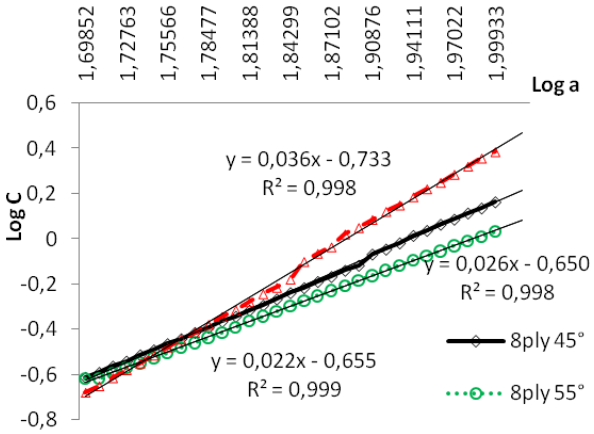

Figure 6. plots of Log C versus log a for 8-ply specimens.

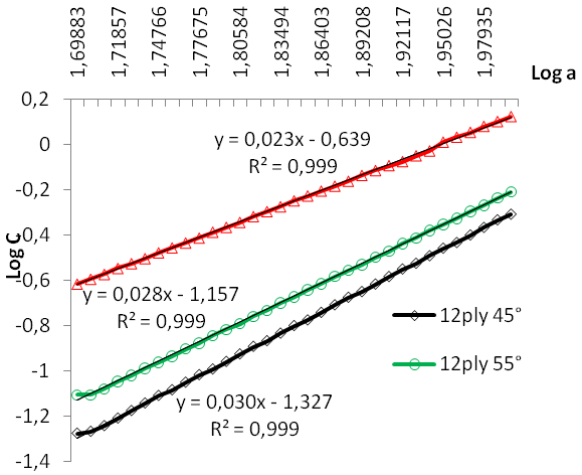

Figure 7.Log C versus log a curves for 12 ply specimens.

Table1. Values of the n and m parameters

	8-ply		12-ply	
	N	**m**	**n**	**m**
[±45°]	1,559	1,97	3,23	4,77
[±55°]	2,594	3,17	3,162	4,44
[±65°]	3,641	4,86	3,25	4,86

3.3 Determination of the critical strain energy release rate GIc

The GIc determined are summarized in Table 2 and plotted in Figure 8 as a function of the number of plies and the winding angles. A closer look at these curves reveals that the strain energy release rate GIc increases with increased winding angle, independent of the number of folds. This means that increasing the winding angle with respect to the propagating crack improves the resistance to delamination. Furthermore, the winding angle of ±65° provides a greater resistance to delamination than those of ±55° and ±45°.

On the other hand, Figure 8, shows that, compared to the 12-ply curve, the 8-ply curve presents higher GIc values whatever the winding angle. This can be explained by the fact that the specimens with 8 ply are less rigid than those with 12 ply, which means that the 8-ply specimens are more vulnerable to bending than delamination. This bending disrupts the tests by consuming more energy in the bending than in delamination. The disturbing bending is increased by an increasing winding angle.

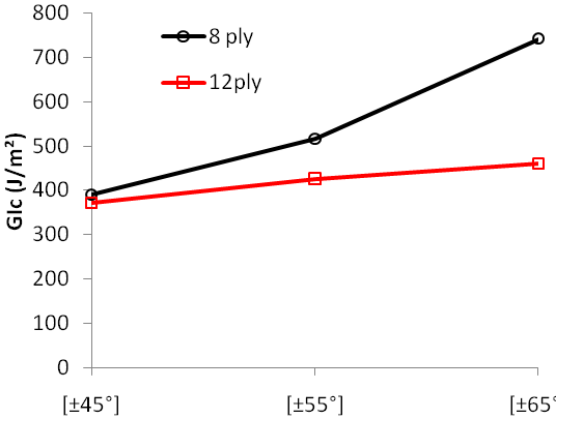

Figure 8.GIc variation function of the number of ply

Table 2. Energy restitution rate GIC for 8-ply corresponding to different orientation angles (±45°, ±55°, ±65°)

	ply	Pc (N)	δ (mm)	C (mm/N)	GIc (J/m²)
±45°	8	28,66	21,93	0,765	390,379
	12	53,19	5,43	0,102	371,671
±55°	8	32,01	15,58	0,486	515,406
	12	54,3	6,22	0,114	425,479
±65°	8	34,79	14,68	0,422	740,845
	12	45,89	7,72	0,168	458,717

3.4 R-curve

The The R-curve describes the failure process through the representation of the variation of the cracking energy as a function of the crack length evolution. The R-curves are plotted according to the variation of the winding angles and the number of piles and are shown in Figure 10. This figure shows that the R-curves have a similar appearance with some disparities in the values. Considering the cracking energy, they show monotonicity followed by an inflection, then a linear growth with a low slope. The monotonicity corresponds to the stability of the fracture behavior with respect to the smooth propagation of the crack. The inflection indicates a transitory behavior inducing an increase in the cracking energy, which is attributed to the bridging of fibers, which consumes more energy. The linearity in the last part of the curves corresponds to the stability of the crack propagation, but the increasing slope reduces its intensity.

Figure 9, shows that the curves related to specimens of 12-ply are lower compared to those of 8-ply. This is mainly due to the effect of bending the strands previously cited, which spend more energy on bending than on cracking for the thinner specimens. Results also show that the number of plies has no effect on the initiation stage, while significantly affecting the propagation stage. Furthermore, the winding angle of 65° provides better delamination resistance behavior than 55° and 45° and is the most vulnerable.

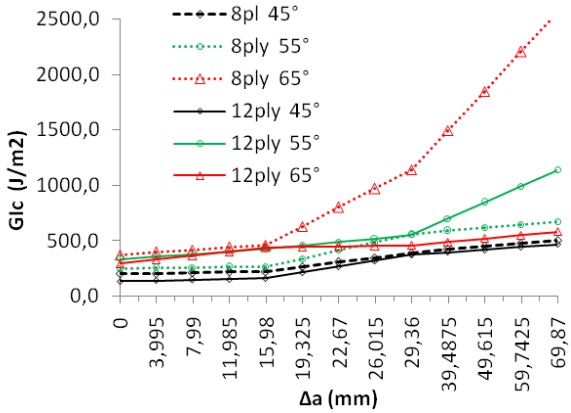

Figure 9. R-curve behavior of 8ply and 12 ply specimens.

3.5 Microscopic observation

A microscopic examination of the fractured areas was conducted, and some micrographs were taken near the crack tips and shown in Figure 10.

As shown in figures 10 A and B, microcracks are observed in the interfacial matrix due to an intra-laminar fracture probably caused by the bending of different plies during loading. With an adequate magnification (Figure 10.C), a plastic deformation in the matrix around the fibers was highlighted. This behavior is attributed to the concentration of an amorphous ductile phase in the fiber-matrix region, which contributes to the improvement of the interfacial bonding by stress transfer from the matrix to the reinforcing fibers. Figure 10D, shows fiber tearing, i.e., decohesion, on both sides of the opening strands. This confirms the formation of fiber bridges previously cited, which act as a reinforcement mechanism against delamination of the material tested.

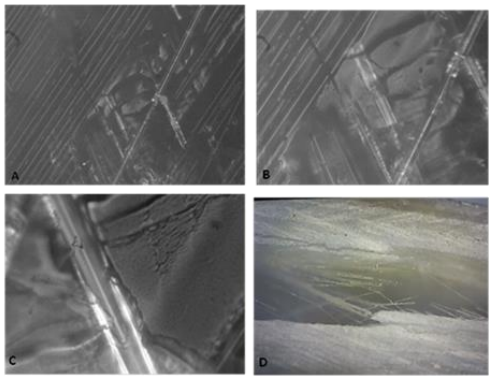

Figure 10.A) Micrographs of fractured surfaces with a magnification of 500x; B): micro cracks formation in the matrix; C): fiber debonding; D): fibre bridging formation.

4 CONCLUSIONS

The effect of fiber orientation angle and number of ply on delamination of commercial glass-fibre-reinforced polymer composite pipes was investigated experimentally. Accordingly, three orientation angles and two plies were chosen in this study. Double cantilever beam specimens with curvature were cut from industrial pipes, and fracture tests in mode-I loading were conducted. Based on the results obtained, the following conclusion can be drawn:

The association of E6 glass fibers (Young's modulus: 81,232 GPa) with the vinyl ester polymer (Young's modulus: 3.3 GPa) allows to obtain a composite material with good properties (Young modulus: 13.2 to 14.3 GPa for composites of 8 ply and up to 20.047 GPa for composites of 12 ply).

The winding procedure used provides a glass volume fraction of about 67.52 percent for composites of 8 ply and 67.64 percent for composites of 12 ply. These values are relatively high compared to the theoretical values provided by piping designers. Although these relatively high values do not affect significantly the mechanical characteristics of the product, it is better to think about optimizing them in order to reduce the production costs.

Increasing the fiber orientation angle as a function of the direction of crack propagation enhances the resistance to delamination independently of the number of folds.

The 65° winding angle provides better delamination resistance than winding angles of 55° and 45°.

The bending of the specimens was identified as a test disturbance affecting the quality of the results. It dissipates a large part of the energy by bending rather than delaminating. Furthermore, its effect increases with an increase in the orientation angle.

The fiber bridging was observed in the wake of the crack-tip. It is considered a reinforcement phenomenon against delamination.

The bending effect can be avoided by increasing the sample's thickness or increasing the number of plies.

To correctly assess the effect of fiber bridging on the delamination, it is suggested to determine the number of fibers engaged in the bridging and measure the bridging force.

The main degradation mode observed was interfacial crack propagation due to bending. It was also observed that the cracks are related to the matrix rather than to fibers. This confirms that the composite studied shows good resistance to the reinforcing fibers.

5 REFERENCES

Sathishkumar. TP. (2014). Glass fiber-reinforced polymer composites – a review, available at: https://doi.org/10.1177/0731684414530790

Baali. B. (2020). Mechanical Characterization and Optimum Design of Wound Glass-Fiber-Reinforced Polymer Pipes Based on the Winding Angle and the Number of Plies, available at: https://link.springer.com/article/10.1007/s11029-020-09912-3

Simon. J-W. (2014). Determination of the initiation of delamination in fiber composites, available at: www.proceedings.blucher.com.br/evento/10wccm.

Nageswara Rao. B. (1995) Maximum load at the initiation of delamination growth in a double cantilever beam specimen, available at: https://doi.org/10.1515/ijmr-1995-860609.

Ghadirdokht. A. (2019). Delamination R-curve behavior of curved composite laminates, available at: https://doi.org/10.1016/j.compositesb.2019.107139.

Raju. S. (2008). Fracture mechanics concepts, stress fields, strain energy release rates, delamination initiation and growth criteria. Edited by: Srinivasan Sridharan; Woodhead Publishing. ISBN 978-1-84569-244-5

Mahmoudi. N. (2014). Effect of volume fiber and crack length on interlaminar fracture properties of glass fiber reinforced polyester composites (GF/PO composites), available at: https://doi.org/10.5755/j01.mech.20.2.6934

Szekrényes. A. (2005). Advanced beam model for fiber-bridging in unidirectional composite double-cantilever beam specimens, available at: https://doi.org/10.1016/j.engfracmech.2005.05.001.

Jia. X., (2013). Effect of geometric factor, winding angle and pre-crack angle on quasi-static crushing

behavior of filament wound CFRP cylinder. Composites Part B: Engineering. Elsevier. ISSN 1359-8368

Rafiee. R. (2013). Experimental and theoretical investigations on the failure of filament wound GRP pipes. Composites Part B: Engineering. Elsevier. ISSN 1359-8368

Yang. W. (2016). Fracture performance of GFRP bars embedded in concrete beams with cracks in an alkaline environment, available at: https://doi.org/10.1061/(ASCE)CC.1943-5614.0000688.

Davies. P. (1994). The effect of defects in tubes: Part 1. Mode I delamination resistance, available at: https://doi.org/10.1007/BF00568040.

Ozdil. F. (1999). Beam analysis of angle-ply laminate mixed-mode bending specimens, available at: http://dx.doi.org/10.1016/S0266-3538(98)00128-6.

Ozdil. F. (2000). Beam analysis of angle-ply laminate mixed-mode bending specimens, available at: https://doi.org/10.1177/002199830003400503

Davies. P. (1989). Interlaminar Mode-I Fracture Testing, Application of Fracture Mechanics to Composite Materials Edited by: K. Friedrich. ISBN: 978-0-444-87286-9

Leonard L.W.H. (2009). Fracture behaviour of glass fibre-reinforced polyester composite, available at: https://doi.org/10.1243/14644207JMDA224.

Setty. M.R. (2000). Effect of fibre orientation on Mode-I interlaminar fracture toughness of glass epoxy composites, available at: https://doi.org/10.1177/073168440001900801.

Mertiny. P. (2004). An experimental investigation on the effect of multi-angle filament winding on the strength of tubular composite structures, available at: DOI:10.1016/S0266-3538(03)00198-2

Julias. A. (2018). Effect of fiber orientation on the delamination behaviour of glass-carbon hybrid interface, available at : http://www.tjprc.org

Davallo. M. (2010). Factors affecting fracture behaviour of composite materials, available at: https://sphinxsai.com/chemtech.php

Aslan. Z. (2020). Experimental determination of residual flexural strength and critical buckling load of impact-damaged glass/epoxy, available at: http://op.niscair.res.in/index.php/IJEMS/issue/view/293.

Wróbel. G. (2017). Influence of the structure and number of reinforcement layers on the stress state in the shells of tanks and pressure pipes, available at: https://doi.org/10.1007/s11029-017-9651-2.

STANDARD, A. S. T. M. (2011). Standard test methods for constituent content of composite materials. D30 Committee.

Rao.D. S. (2017). P.R. Determination of mode-I fracture toughness of epoxy-glass fibre composite laminate, available at: https://doi.org/10.1016/j.proeng.2016.12.193

Suresh. G. (2016). Analyzing the mechanical behavior of E-glass fibre-reinforced interpenetrating polymer network composite, available at: https://doi.org/10.1177/0021998315615408.

Prasad. M.S.S. (2011). Experimental methods of determining fracture toughness of fiber reinforced polymer composites under various loading conditions, available at: http://jmmce.org/

Gunderson. J.D. (2007), Alternative test method for interlaminar fracture toughness of composites, available at: https://doi.org/10.1007/s10704-007-9063-8.

.

6 NOTATION

The following symbols are used in this paper:
P = the load,
δ = the load line deflection,
a = the crack length,
b = the beam width are,
aeff = the effective crack length,
Gip = the interlaminar propagation energy,
m and n = the intrinsic constants of the material,
GIc = the critical energy release rate for the opening loading mode
C= Compliance
GIIc = the critical energy release rate for the forward shear loading mode
GIIIc = the critical energy release rate for the anti-plane shear mode

Data Availability Statement: Some or all data, models, or code that support the findings of this study are available from the corresponding author upon reasonable request.

Funding: The author(s) received no specific funding for this work.

Conflict of interest: The authors declare that they have no conflict of interest